TECHNICAL REPORT ARCCB-TR-01018

FAILURE BENEATH CANNON THERMAL BARRIER COATINGS BY HYDROGEN CRACKING; MECHANISMS AND MODELING

20011003 045

JOHN H. UNDERWOOD
GREGORY N. VIGILANTE
EDWARD TROIANO

SEPTEMBER 2001

APPROVED FOR PUBLIC RELEASE; DISTRIBUTION UNLIMITED

REPORT DOCUMENTATION PAGE

1. AGENCY USE ONLY (Leave blank)	2. REPORT DATE	3. REPORT TYPE AND DATES COVERED
	September 2001	Final

4. TITLE AND SUBTITLE

FAILURE BENEATH CANNON THERMAL BARRIER COATINGS
BY HYDROGEN CRACKING; MECHANISMS AND MODELING

5. FUNDING NUMBERS

AMCMS No. 6226.24.H180.0
PRON No. TU1E1F261ABJ

6. AUTHOR(S)

John H. Underwood, Gregory N. Vigilante, and Edward Troiano

7. PERFORMING ORGANIZATION NAME(S) AND ADDRESS(ES)

U.S. Army ARDEC
Benet Laboratories, AMSTA-AR-CCB-O
Watervliet, NY 12189-4050

8. PERFORMING ORGANIZATION REPORT NUMBER

ARCCB-TR-01018

9. SPONSORING / MONITORING AGENCY NAME(S) AND ADDRESS(ES)

U.S. Army ARDEC
Close Combat Armaments Center
Picatinny Arsenal, NJ 07806-5000

10. SPONSORING / MONITORING AGENCY REPORT NUMBER

11. SUPPLEMENTARY NOTES

Presented at the 33rd National Symposium on Fatigue and Fracture Mechanics, Moran, WY, 26-29 June 2001.
Published in ASTM STP 1417.

12a. DISTRIBUTION / AVAILABILITY STATEMENT

Approved for public release; distribution unlimited.

12b. DISTRIBUTION CODE

13. ABSTRACT (Maximum 200 words)

Army experience with hydrogen cracking failures of cannons is described, including extensive testing of high-strength steel and nickel-iron base alloys to address the failures. Cracking of cannon pressure vessel steels just under bore thermal barrier coatings is now common, and can be explained by the combined action of hydrogen-bearing combustion gases and thermally induced tensile residual stresses. Above-yield transient thermal compression and resultant residual tension stresses beneath the coating are shown to give good predictions of crack arrays observed under the coatings. A similar array of hydrogen cracks in a prototype cannon has recently been explained by contact of combustion gases with uncoated high-strength steel that has been yielded by mechanical compressive stresses, leading to residual tension and cracking. The use of nickel-plated hydrogen barrier coatings was shown to eliminate this type of cracking.

Recent cannon experience provides a basis for a summary of mechanisms of hydrogen cracking beneath cannon barrier coatings. The near-bore transient temperature distributions due to cannon firing are calculated by finite-difference calculations using temperature-dependent thermal and physical properties and validation by comparison with the known temperatures and the observed depths of microstructural damage. Solid mechanics calculations of transient thermal compressive stresses and resultant residual tensile stresses are made, taking account of temperature-dependent coating properties and yielding of the steel substrate near the bore surface. Effects of coating material, coating thickness, and the temperature and duration of firing gases on the depth of thermal damage below the coating are investigated. Direct comparisons between observed and predicted thermal damage and hydrogen cracking are made for coating and firing conditions that correspond to modern cannon firing. This comparison suggests changes in cannon bore coatings to handle the more extreme thermal conditions in modern cannon firing, including thicker or more durable thermal barrier coatings to minimize thermal stresses in the steel substrate and different coating materials that can serve as hydrogen barrier coatings.

14. SUBJECT TERMS

Thermal Stress, Residual Stress, Hydrogen Cracking, Thermal Barrier Coating, Cannon Tube, High-Strength Steel, Thermomechanical Model

15. NUMBER OF PAGES

18

16. PRICE CODE

17. SECURITY CLASSIFICATION OF REPORT	18. SECURITY CLASSIFICATION OF THIS PAGE	19. SECURITY CLASSIFICATION OF ABSTRACT	20. LIMITATION OF ABSTRACT
UNCLASSIFIED	UNCLASSIFIED	UNCLASSIFIED	UL

TABLE OF CONTENTS

TABLES

LIST OF ILLUSTRATIONS

DEDICATION AND ACKNOWLEDGEMENT

INTRODUCTION

Damage near the bore surface of a fired cannon can take many forms. Mechanically induced yielding or fatigue cracking due to the gas pressure often start at the bore, but these types of damage are not considered here. Thermally induced expansion or phase transformation of a shallow bore layer will occur if there is sufficient temperature and duration of the pulse of hot firing gases. Environmentally induced cracking or other damage will occur if an aggressive chemical species is present for the required combination of time and temperature. To help cope with these various forms of firing damage, a protective coating is often applied to cannons, typically a 0.1 to 0.2-mm thick electroplated layer of chromium. As cannon gas pressures and temperatures have increased, the depth and degree of bore damage have likewise increased. One particular type of cannon bore damage is now observed that is closely involved with each of the three forms of damage mentioned above and deserves special attention: thermally induced expansion of a bore layer is observed to cause compressive yielding and associated tensile residual stress, which in turn causes environmental cracking and premature erosion and fatigue failure of the cannon.

The objectives here are:

- To briefly review the recent investigations that support this *thermal expansion–residual stress–environmental cracking* damage scenario
- To use thermomechanical modeling to characterize the controlling parameters of this type of thermally-initiated damage, including the thickness and material type of the protective coating and the temperature and time duration of the pulse of hot gases at the cannon bore

RECENT INVESTIGATIONS

Thermally Induced Environmental Cracking

The extreme sensitivity of cannon systems to environmental cracking, particularly hydrogen cracking, has fostered a considerable amount of crack growth testing with the high-strength alloys and hydrogen environments typical of cannon applications. Vigilante et al. (refs 1,2) have tested a variety of high-strength steel and nickel-iron base alloys in electrolytic cell and acid hydrogen environments using automated crack-growth methods with a bolt-load compact specimen incorporating an instrumented-bolt. Their most striking finding in relation to the alloy steels used for cannons was their extreme sensitivity to hydrogen cracking at yield strengths of 1100 MPa and above. A 20% increase in yield strength, from 1145 to 1380 MPa, yielded a *thousand-fold* increase in crack growth rate in carefully controlled laboratory tests. Current work (ref 3) has shown a further hundred-fold increase in crack growth rate for 1310 MPa yield alloy steel in a different acid hydrogen environment from that of earlier tests. These results help provide an explanation and background for the upcoming descriptions of hydrogen cracking events in fired cannons.

One particular aspect of cracking that has been observed recently in fired cannons provides a simple yet compelling argument for the importance of hydrogen cracking in cannons. The expected type of mechanical fatigue cracking in a cannon is the C-R orientation shown in Figure 1, with initially a few and then later one dominant crack growing in the plane normal to the circumferential (i.e., hoop) stress, the dominant applied stress in a pressure vessel. However, an extensive array of nearly constant-depth C-R cracks has often been observed in fired tubes, particularly tubes that have experienced a relatively high firing gas temperature. Moreover, the C-R cracks are accompanied by an array of L-R cracks normal to the axial direction with a larger depth than that of the C-R cracks. A deep array of L-R cracks simply cannot be explained by a mechanical fatigue process. A cannon, being an open-end pressure vessel, has no significant axial firing stress that could grow L-R fatigue cracks. This and other unanswered questions led Underwood et al. (refs 4,5) to investigate other causes and consequences of these arrays of constant-depth cracks that are observed in fired cannons.
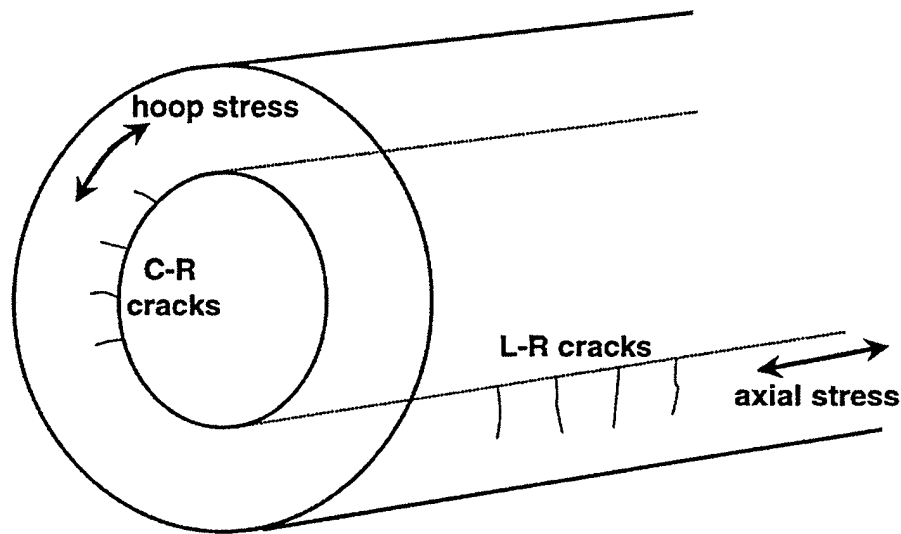
Figure 1. Cracking observed at bore of fired cannon.

The typical appearance of an array of L-R cracks and other damage at the bore of a fired cannon is considered next; see Figure 2. A longitudinal metallographic section is shown from a cannon with a 0.12-mm chromium coating, after 40 experimental firings with a relatively high gas temperature. Key features from the top surface of the coating downward into the steel are (ref 4):

- An extensive array of cracks that grow completely around the cannon bore surface, through the coating and into the steel with an intergranular appearance to an average total depth of 0.46-mm
- Recrystallization and grain growth (to about 0.01-mm grain diameter) of the chromium coating to an average depth of 0.08-mm, corresponding to a temperature of about 1320°K

- Transformation of the A723 steel to an average depth of 0.07-mm below the chromium-steel interface for a total depth of 0.19-mm below the surface, corresponding to the 1020°K phase transformation temperature

These damage features, including chromium and steel cracking, chromium recrystallization, and steel transformation, have been observed before (ref 6), although not nearly to the degree observed here because of the higher gas temperatures in this work. Related damage concerns, such as the volumetric expansion of the steel transformation and the effect of time at temperature on steel transformation, have been discussed in earlier work (ref 4). The volumetric expansion of transformation is considerably smaller than the thermal expansion, and the few milliseconds time at temperature of cannon firing was thought to be sufficient for the steel transformation to occur. Recent results using pulsed laser heating of coated steel samples (ref 7) have confirmed the time-at-temperature question.
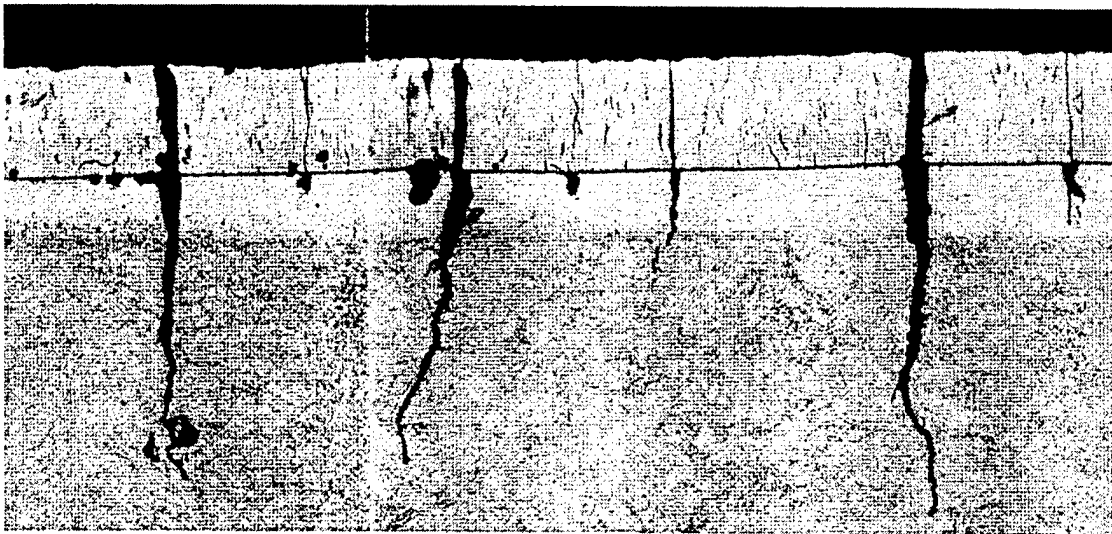
Figure 2. Longitudinal section of fired cannon bore showing thermal damage and L-R cracking in chromium plate and underlying A723 steel (100X).

The damage feature most difficult to ignore is the deep cracks through and under the coating, since the cracks critically undermine the coating, as described in Reference 5. The observed damage and model calculations from prior work (refs 4,5) can be used to identify the basic cause of the arrayed cracks and also to obtain quantitative descriptions of factors that control the degree of cracking. Regarding the basic cause, environmental cracking is considered much more likely than fatigue cracking, based on the following considerations:

- The appearance of intergranular cracking in Figure 2
- The lack of a significant axial direction fatigue stress
- The close proximity of constant-length cracks
- The small number of firings experienced
- The extreme sensitivity of A723 steel to hydrogen cracking

3

- The significant concentration of hydrogen in cannon firing gases, believed to be as high as 10%.

Regarding factors that can control this type of thermal-damage cracking, the observed chromium recrystallization and steel transformation temperatures provide direct verification of the critical information required for describing thermal damage—the near-bore temperature distribution. Knowledge of temperatures directly within the area of thermal damage provides important validation of the thermal damage model used to determine the controlling factors of thermal damage. This is described in upcoming results.

Mechanically Induced Environmental Cracking

One further recent investigation that clearly addresses both the cause and the controlling factors of cannon firing damage is the work of Troiano et al. (ref 8). They observed very fast formation of an array of cracks in a maraging steel piston that sealed the breech end of a pressure vessel subjected to simulated cannon firing. The piston was subjected to the same hydrogen-containing combustion gas and similar gas temperature and pressure as those of gun firing. However, there was very little gas flow over the piston, so the piston surface suffered little thermal damage. The pressure on the piston did result in above-yield-level compression stress at the surface of the piston, as verified by permanent concave 'dishing' of the piston surface that is exposed to firing pressure. The exposed surface developed an array of cracks following a few firings (as few as two), and the cracks could be seen with the unaided eye, Figure 3a. Typically, the cracks were up to 20-mm long and spaced about 10-mm apart. A crack was broken open and viewed by scanning electron microscopy (SEM) to reveal the fracture appearance; see Figure 3b. Evidence of ductile fracture can be seen at the lower right, where the specimen was broken open after removal from the cannon. Most of the surface, although partially obscured by what is believed to be reaction product, showed the characteristic intergranular appearance of hydrogen cracking. These classic intergranular cracks, observed following cannon firing that involved unambiguous mechanical compressive yielding and hydrogen access, provide strong support for the *thermal expansion–residual stress–environmental cracking* damage scenario discussed earlier. Clear evidence of hydrogen cracking due to mechanically induced tensile residual stress supports the contention that thermally induced tensile residual stress is the cause of hydrogen cracking beneath cannon thermal barrier coatings. In the next sections of this work thermomechanical modeling will be used to characterize the controlling parameters of this type of cracking in cannons.
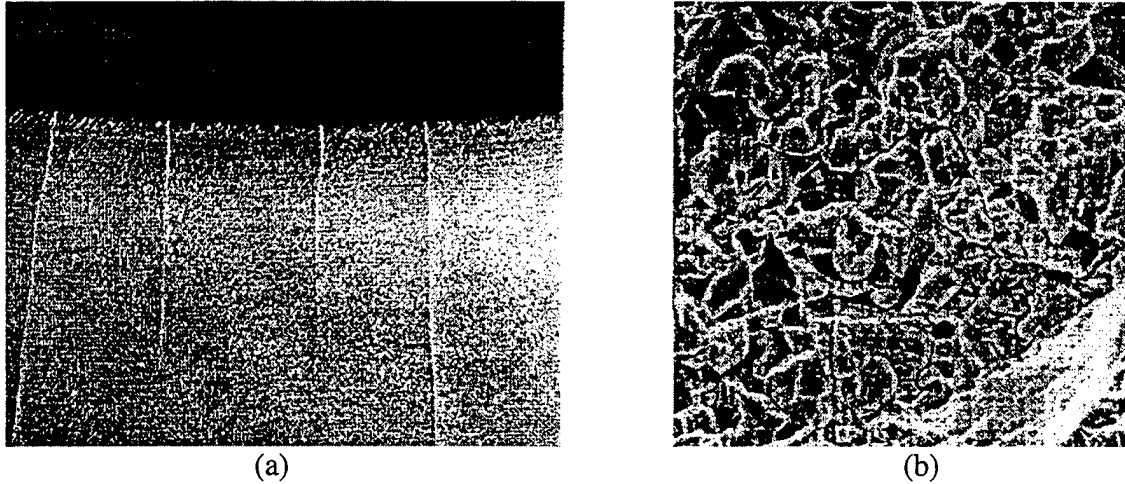
Figure 3. Hydrogen cracking observed in cannon component showing (a) macrograph of surface at 2X, and (b) SEM fractograph of opened crack at 400X.

THERMOMECHANICAL MODEL

Many of the model concepts are described in prior work (refs 4,5,9), so only a summary of procedures is given here. The basis of the modeling is the near-bore temperature distribution, obtained by finite-difference temperature calculations in Reference 4, an approximate expression in Reference 5, and most recently, and in this work, by finite-difference calculations in a convenient spread-sheet form in Reference 9. For the work here, finite-difference calculations of one-dimensional convective heat flow were used to determine the near-bore temperatures produced by cannon firing conditions. The calculations used increments of about 0.02-mm in depth below the heated bore surface. About fifty increments were required for the temperature to drop from typically 1500°K at the surface to within 1°K of ambient at about 1-mm below the surface, for the few ms of convective heating typical of cannon firing. Temperature-dependent material properties (refs 10-12) of chromium, molybdenum, and tantalum coatings and the A723 steel substrate were used for the analysis, in the form $fn(T) = C_0 + C_1T$; see Table 1. The inputs to the finite-difference calculations, in addition to the chromium and steel properties, were:

- The thickness of the coating, typically 0.1 to 0.2-mm
- The initial ambient temperature, $T_i = 300°K$
- The duration of the convective heating pulse at the tube surface, 0.005 to 0.016-s
- The convection coefficient of the heating pulse, $h = 193{,}000 \ W/m^2 \ °K$
- The mean gas temperature of the pulse, T_{GAS}, with values as discussed in the upcoming results.

Expressions for the near-bore, transient, in-plane, biaxial compressive thermal stress, S_T, and the tensile residual stress, S_R, produced in the steel substrate when the transient stress exceeds the steel yield strength, are as follows:

5

$$S_T = -E\alpha[T\{x,t\} - T_i]/[1 - v] \qquad (1)$$

$$S_R = -S_T - S_Y \qquad for\ S_T > S_Y \qquad (2)$$

where v is Poisson's ratio; the transient temperature, T, from the finite-difference calculations is for a given depth, x, below the bore surface and duration, t, of a heating pulse; the term $[1 - v]$ accounts for the biaxial nature of the temperature and stress distributions. The value of S_R is determined using the linear unloading concept, in which a residual stress is created by a virtual unloading from a calculated elastic applied stress (thermal in this case) that is envisioned to be above the yield level of the material. The residual stress is of opposite sense to the applied stress and of a value equal to the difference between the applied stress and the yield strength, as shown by equation (2).

Table 1. Temperature-Dependent Properties of Coatings and Substrate

	Thermal Diffusivity $\delta, m^2/s$		Thermal Conductivity $k, W/m\,°K$		Elastic Modulus E, GPa		Thermal Expansion $\alpha, 1/°K$	
Valid For:	C_0 (300-2000°K)	C_1	C_0 (300-2000°K)	C_1	C_0 (300-1000°K)	C_1	C_0 (300-1000°K)	C_1
Chromium	29.6E-6	-12.6E-9	97.2	-0.0266	--	--	--	--
Molybdenum	56.3E-6	-17.8E-9	144	-0.0291	--	--	--	--
Tantalum	25.1E-6	-1.20E-9	56.3	-0.0039	--	--	--	--
Steel	11.7E-6	-5.30E-9	43.6	-0.0097	248	-0.097	13.5E-6	0

It is important to account for the change in the steel yield strength with temperature when calculating residual stress using equation (2). If the room temperature value of strength were used, an underestimate of the tensile residual stress and its depth would result. Yield strength as a function of test temperature is available for AISI 4340 steel (ref 10), and this provides a close measure of the temperature-dependent strength for cannon steel. Using these results, the following expression was developed for use with equation (2) to account for the effect of temperature-dependent yielding on the tensile residual stress in the steel beneath the coating:

$$S_Y = S_{Y-RT}(1.32 - 0.00105T) \qquad (3)$$

where S_{Y-RT} is the room temperature yield strength of steel, 1100 MPa in this case, and T is temperature in °K. This approach was used in the model results, considered next.

MODEL RESULTS

Representative Temperatures and Stresses

Model calculations of near-bore temperatures and transient and residual stresses have been performed for various cannon firing conditions. Some measure of the reliability of these calculations can be obtained by comparison with the results of Perl and Ashkenazi (ref 13). They used a finite element method to calculate temperatures at and below the bore surface of an all-steel cannon with $T_{GAS} = 3000°K$, $T_i = 294°K$, $h = 145,200\ W/m2\ °K$, $\delta = 12.5E-6\ m^2/s$, $k = 45.2\ W/m\,°K$, and various heating time durations, Δt. Their calculated bore temperature for $\Delta t =$

6

0.008-s is about 1850°K, compared with the bore temperature from our finite-difference method for the same inputs, 1880°K. This close agreement, within 2%, provides independent verification of the methods and results here.

The calculated temperature and stress distributions for the cannon with 40 experimental firings discussed earlier in reference to Figure 2 are shown in Figure 4. The finite-difference calculations used the following inputs:

- The chromium and steel properties from Table 1
- A 0.12-mm thick chromium coating
- $T_i = 300°K$; $h = 193,000$ $W/m2$ $°K$; $t = 0.008$-s; and mean $T_{GAS} = 2160°K$

These input values are believed to represent an upper limit of the relatively severe thermal conditions expected in modern cannons, and will serve as a basis of comparison in the results here. The maximum calculated temperature distribution drops from 1480°K at the bore surface, passes near the approximate 1320°K chromium recrystallization temperature (ref 4) at the 0.08-mm observed depth, changes slope as expected at the chromium-steel interface at 1240°K, and agrees closely with the most reliable validation point, the 1020°K steel transformation temperature at the 0.19-mm observed depth. Considering the good agreement between the calculations and the observed chromium and steel metallographic transformations, these calculated temperatures provide a sound basis for determining the transient and residual stresses in the near-bore region of a fired cannon. The baseline temperatures can be compared with those calculated from an erosion model of cannon firing with a new high gas-temperature tank round (ref 14). This gave bore and interface temperatures of about 1560 and 1240°K, which are 6% above and within 1% of the values here, respectively. This is considered to be very good agreement.
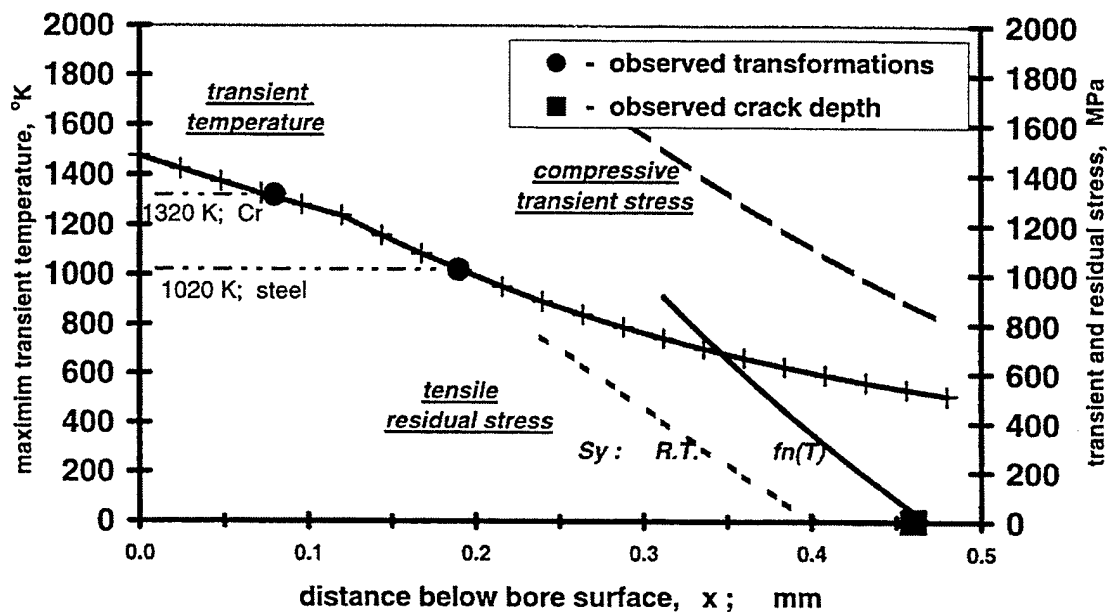
Figure 4. Transient temperatures and resultant stresses in a fired cannon with 0.12-mm chromium plate, $\Delta t = 0.008$-s, and mean $T_{GAS} = 2160°K$.

7

Referring again to Figure 4, the transient compressive stress and residual tensile stress distributions based on the calculated temperatures are shown in the plot, along with the temperatures. Note that upon the inclusion of the temperature variation of yielding modification in the residual stress [using equation (3)], the distribution shifts considerably deeper. As would be expected, the reduced yield strength at elevated temperature results in a deeper penetration of residual stresses. It is suggested here that the point at which the tensile residual stress reaches zero may be a useful prediction of the depth of hydrogen cracking. This is consistent with the very low threshold stress for hydrogen cracking observed by Vigilante et al. (refs 1,2). This premise results in good agreement between observed crack depth and the predicted depth (at zero residual stress), and it is consistent with a moderate reduction in the steel yield strength due to its brief exposure to elevated temperature during cannon firing. This approach will be used in all upcoming results.

Parameters Controlling Damage and Cracking

The remaining figures present model results that show effects of key physical parameters on the degree of thermal damage and cracking in the near-bore region of a fired cannon. Figure 5 shows the effect of the type of coating material on the temperatures within and below a 0.12-mm thick coating, with the other control parameters unchanged from those discussed in relation to Figure 4. The 4% higher bore temperature for tantalum (1540°K) compared with that for chromium and molybdenum (1480°K) and the 5 to 8% higher interface temperature for molybdenum (1330°K) compared with those for chromium and tantalum are the result of the different δ and k values for the various materials in this range of temperature. In general, however, the differences in calculated temperature are relatively small for a 0.12-mm thick coating of these three materials. It is clear that thin coatings of good conducting metals can have only small effects on near-bore cannon temperatures. This relative insensitivity to temperature differences is also reflected in the values of residual stress. No significant differences are noted in the residual stress distributions for the three coating materials. Thus, the predicted depth of hydrogen cracks for molybdenun and tantalum coatings (determined for $S_R = 0$) are not much different from that predicted for chromium, or from that observed for chromium, 0.46-mm.
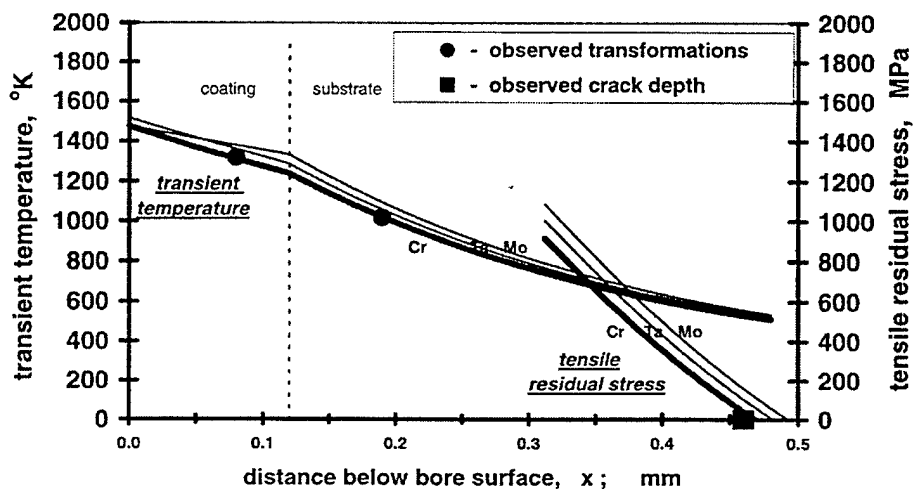
Figure 5. Calculated temperature and residual stress for various materials with 0.12-mm thick coatings, $\Delta t = 0.008$-s, and mean $T_{GAS} = 2160$°K.

The effect of thickness of a chromium coating on thermal damage and cracking is considered next; see Figure 6. Comparing the bore temperature results for the 0.12-mm thick chromium coating with results for 50 and 100% increases in coating thickness shows little change, only about 1 and 2% decreases in bore temperature, respectively. This can be understood by considering that the thermal properties of chromium and steel in this temperature range are quite similar, so the temperature at any given location in the coating, such as the coating surface in this case, will vary little with coating thickness. Comparing the interface temperatures shows much more effect of coating thickness, with 10 and 18% decreases in interface temperature for 50 and 100% increases in coating thickness, respectively. In this case three different locations below the bore surface are being compared, and the steep temperature gradient results in noticeable differences in temperature among the three locations. Finally, comparing a subinterface temperature, such as at 0.25-mm below the bore surface, shows a moderate *increase* in temperature with an increase in coating thickness. This result may at first seem counter-intuitive, but it can be understood by noting that chromium is somewhat less able to dissipate the heat from the bore surface, as shown by the noticeably shallower chromium temperature gradient compared with that for steel. The lower dissipation of heat for chromium leads to an increase in temperature for thicker chromium coatings. Note that the increased subinterface temperature for thicker chromium leads to increases in depth of tensile residual stress, and thus an increase in the predicted depth of hydrogen cracking. The increases in temperature, residual stress, and crack depth for thicker coatings are moderate, because of the moderate differences in properties noted earlier. Nevertheless, the increased temperature and its effects are clearly expected for a coating that dissipates heat less well than the substrate.
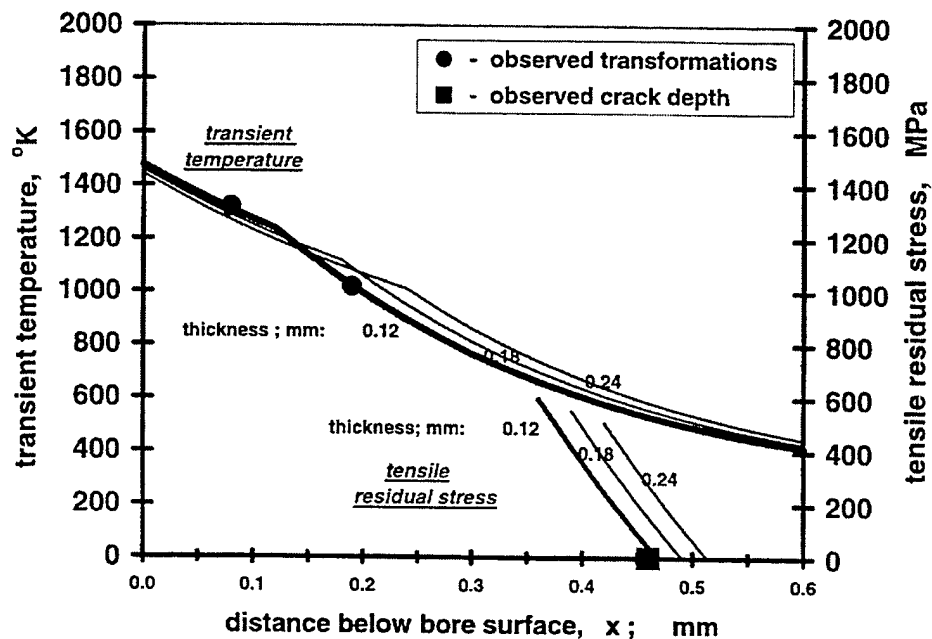
Figure 6. Calculated temperature and residual stress for various chromium coating thicknesses with Δt = 0.008-s and mean T_{GAS} = 2160°K.

9

The effect of the duration of the firing heat pulse on thermal damage and cracking is considered next; see Figure 7. Durations of $t = 0.005$-s and 0.012-s were modeled (with other controls held constant), for comparison with the base value of 0.008-s. A review of Figures 5 through 7 shows that heating duration has a greater effect on thermal damage and cracking than do the material or thickness of the coating. Considering specific results, the 50% increase in heating duration (from 0.008 to 0.012-s) resulted in a 7% increase in bore temperature, a 10% increase in interface temperature, and a 23% increase in expected depth of hydrogen cracking. Figure 7 also shows that the advantages of shorter heating duration are very significant, based on the large decreases in temperature and residual stress predicted for a significant decrease in duration. It is clear that duration of heating pulse during cannon firing exerts significant control over the thermal damage and associated hydrogen cracking.
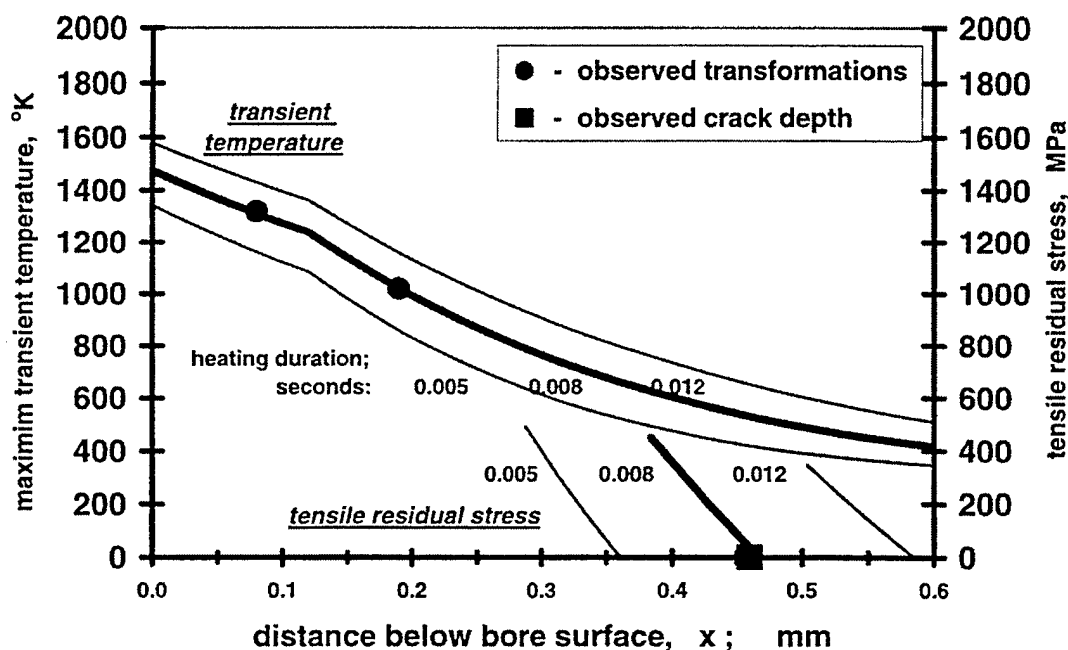
Figure 7. Calculated temperature and residual stress for various heating durations with 0.12-mm thick chromium coatings and mean $T_{GAS} = 2160°K$.

Finally, the effect of mean gas temperature on thermal damage and cracking is considered; see Figure 8. Gas temperatures of 25 and 50% above the 2160°K base value were considered. The effect of gas temperature was more pronounced near the bore surface, as can be appreciated by comparing Figures 7 and 8. The effect of heating duration, summarized in Figure 7, was seen at all depths, whereas the gas temperature effects diminished somewhat at locations farther below the surface in Figure 8. From specific results, the 50% increase in gas temperature resulted in 44 and 34% increases in bore and interface temperatures, respectively, and in a 13% increase in expected depth of hydrogen cracking. In all cases, higher gas temperature resulted in deeper predicted crack depth. This is as expected, because higher temperatures lead to compressive yielding and tensile residual stress at a greater depth, and thus cracks grow deeper. It is clear that mean gas temperature has direct and predictable control over the near-bore thermal damage and associated hydrogen cracking resulting from cannon firing.
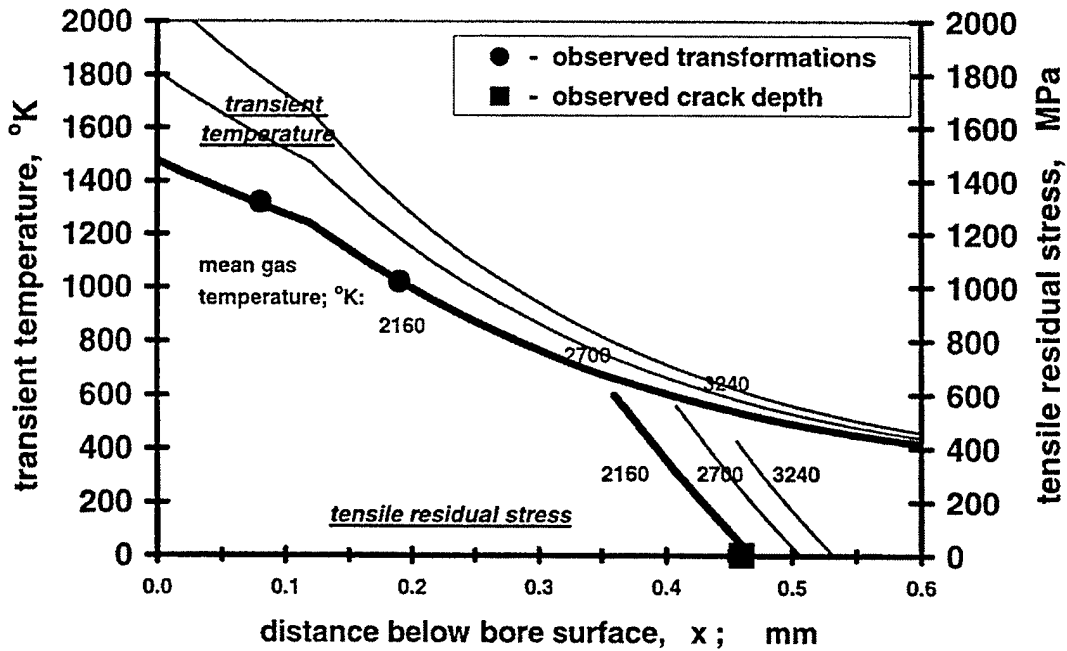
Figure 8. Calculated temperature and residual stress for various gas temperatures with 0.12-mm thick chromium coatings and Δt = 0.008-s.

Sensitivity Analysis of Controlling Parameters

A useful summary and comparison of the controlling parameters for thermally-initiated cannon bore damage is a sensitivity analysis of the parameters considered. This has been done and is listed in Table 2 as simply the percent change in model temperatures and crack-depth predictions for specified changes in the identified control parameters. The parameters and the changes considered are:

- Coating material (chromium, molybdenum, tantalum)
- Coating thickness (50% increase)
- Heating pulse duration (50% increase)
- Mean gas temperature (50% increase)

The 50% increase in the various control parameters may not be realistic in some cases, but it does provide a common basis of comparison. The subinterface temperature results shown are at an arbitrary depth of 0.25-mm below the cannon bore surface, below the coating-steel interface in all cases.

11

**Table 2. Sensitivity Analysis for Controlling
Parameters of Cannon Thermal Damage**

	Bore Temperature (% Change)	Interface Temperature (% Change)	Subinterface Temperature (% change)	Predicted Crack Depth (% Change)
Coating Material				
Molybdenum Versus Chromium	0%	+8%	+7%	+5%
Tantalum Versus Chromium	+4%	+3%	+3%	+3%
Chromium Coating Thickness				
0.18 Versus 0.12-mm	-1%	-10%	+11%	+5%
Heating Duration				
0.012 Versus 0.008-s	+7%	+10%	+16%	+23%
Gas Temperature				
3240 Versus 2160°K	+44%	+34%	+26%	+13%

A review of Table 2 shows that gas temperature has far more control over thermal damage and cracking in fired cannons than other parameters, as might have been expected. Second in importance in control of damage is the duration of the pulse of gas temperature, which becomes relatively more important for the deeper subinterface area and the predicted crack depth that is related to the subinterface area. Coating thickness and coating material are the least important of the control parameters considered in the modeling, since they typically resulted in 5 to10% predicted change in near-bore temperatures and crack depth, whereas gas temperature and duration typically resulted in 10 to 40% predicted change in near-bore temperatures and crack depth.

CONCLUSIONS

The key conclusions from this study of cannon bore thermal damage and cracking can be divided into two categories: mechanisms and modeling methods, and characterization of damage control parameters.

Regarding mechanisms and modeling of cannon thermal damage, this study shows:

- The damage mechanism involving *thermal expansion–residual stress–environmental cracking* of the near-bore region of a fired cannon is validated by recent observations of hydrogen cracking in cannons following thermally or mechanically induced compressive yielding.

- A thermomechanical model using the finite-difference calculation of transient temperature with temperature-dependent thermal properties and solid mechanics calculations of transient thermal stress and residual stress with account for yielding gives a good representation of near-bore thermal damage in a fired cannon. The model temperatures agree well with observed depths and known temperatures of steel and chromium metallographic transformations.

Regarding characterization of the key control parameters for cannon thermal damage, this study shows:

- In general, the gas temperature and its time duration have significant control over near-bore transient temperatures and subinterface stresses, whereas the type of coating and its thickness are of secondary importance.

- Increased thickness coatings of metals with poorer heat dissipation than the substrate result in a slight decrease in bore temperature, a significant decrease in interface temperature, and a significant increase in subinterface temperature and associated tensile residual stress and hydrogen cracking.

- A 0.12-mm-thick metal coating has limited use as a thermal barrier coating in cannons, because it has little effect on temperatures and associated thermal damage in the near-bore region of a fired cannon.

- A 0.12-mm-thick metal coating has potential use as a hydrogen barrier coating in high-temperature cannon firing provided it limits diffusion of hydrogen and resists failure by thermal expansion stresses.

REFERENCES

1. Vigilante, G.N., Underwood, J.H., Crayon, D., Tauscher, S., Sage, T., and Troiano, E., "Hydrogen Induced Cracking Tests of High-Strength Steels and Nickel-Iron Base Alloys Using the Bolt-Loaded Specimen," *Fatigue and Fracture Mechanics: 28th Volume, ASTM STP 1321,* 1997, pp. 602-616.

2. Vigilante, G.N., Underwood, J.H., and Crayon, D., "Use of the Instrumented Bolt and Constant Displacement Bolt-Loaded Specimen to Measure In-Situ Hydrogen Crack Growth in High-Strength Steels," *Fatigue and Fracture Mechanics: 30th Volume, ASTM STP 1360,* 1999, pp. 377-387.

3. Troiano, E., Vigilante, G.N., and Underwood, J.H., "Experiences and Modeling of Hydrogen Cracking in a Thick-Walled Pressure Vessel," *Fatigue and Fracture Mechanics: 33rd Volume, ASTM STP 1417,* American Society for Testing and Materials, West Conshohocken, PA, 2002, in review.

4. Underwood, J.H., Parker, A.P., Cote, P.J., and Sopok, S., "Compressive Thermal Yielding Leading to Hydrogen Cracking in a Fired Cannon," *Journal of Pressure Vessel Technology,* Vol. 121, 1999, pp.116-120.

5. Underwood, J.H., and Parker, A.P., "Thermal Damage and Shear Failure of Chromium Plated Coating on an A723 Steel Cannon Tube," *Journal of Pressure Vessel Technology,* 2001, to be published.

6. Turley, D.M., "Erosion of a Chromium-Plated Tank Gun Barrel," *Wear,* Vol. 131, 1989, pp. 135-150.

7. Cote, P. J., Kendall, G., and Todaro, M., "Laser Pulse Heating of Gun Bore Coatings," *Surface Coatings and Technology,* 2001, to be published.

8. Troiano, E., Vigilante, G.N., Underwood, J.H., and Mossey, C., "Analysis of a Piston Experiencing Environmentally-Assisted Cracking as a Result of Compressive Overloading," *Progress in Mechanical Behaviour of Materials, ICM8,* Fleming Printing Ltd., Victoria, BC, Canada, 1999, pp. 603-608.

9. Underwood, J.H., Parker, A.P., Troiano, E., Vigilante, G.N., and Witherell, M.D., "Fatigue and Hydrogen Cracking in Cannons with Mechanical and Thermal Residual Stress," *Proceedings of 10th International Conference of Fracture,* 2001, to be published.

10. Incropera, F.P., and DeWitt, D.P., *Introduction to Heat Transfer,* Wiley, NY, 1985, pp. 669-672.

11. Brown, W.F., Jr., ed., *Aerospace Structural Metals Handbook, Volume IIA, Non-Ferrous Alloys,* Mechanical Properties Data Center, Traverse City, MI., 1970.

12. Smithells, C.J., *Metals Reference Book*, Butterworths, Washington, 1962.

13. Perl, M., and Ashkenazi, A., "A More Realistic Thermal Shock Analysis of a Radially Multicracked Thick-Walled Cylinder," *Engineering Fracture Mechanics*, Vol. 42, 1990, pp. 747-756.

14. Sopok, S., and Fleszar, M., "Ablative Erosion Model for the M256/M829E3 Gun System," *Proceedings of 37th JANNAF Combustion Meeting*, Monterey, CA, 13-17 November 2000.

TECHNICAL REPORT INTERNAL DISTRIBUTION LIST

	NO. OF COPIES
TECHNICAL LIBRARY ATTN: AMSTA-AR-CCB-O	5
TECHNICAL PUBLICATIONS & EDITING SECTION ATTN: AMSTA-AR-CCB-O	3
OPERATIONS DIRECTORATE ATTN: SIOWV-ODP-P	1
DIRECTOR, PROCUREMENT & CONTRACTING DIRECTORATE ATTN: SIOWV-PP	1
DIRECTOR, PRODUCT ASSURANCE & TEST DIRECTORATE ATTN: SIOWV-QA	1

NOTE: PLEASE NOTIFY DIRECTOR, BENÉT LABORATORIES, ATTN: AMSTA-AR-CCB-O OF ADDRESS CHANGES.

TECHNICAL REPORT EXTERNAL DISTRIBUTION LIST

	NO. OF COPIES		NO. OF COPIES
DEFENSE TECHNICAL INFO CENTER ATTN: DTIC-OCA (ACQUISITIONS) 8725 JOHN J. KINGMAN ROAD STE 0944 FT. BELVOIR, VA 22060-6218	2	COMMANDER ROCK ISLAND ARSENAL ATTN: SIORI-SEM-L ROCK ISLAND, IL 61299-5001	1
COMMANDER U.S. ARMY ARDEC ATTN: AMSTA-AR-WEE, BLDG. 3022 AMSTA-AR-AET-O, BLDG. 183 AMSTA-AR-FSA, BLDG. 61 AMSTA-AR-FSX AMSTA-AR-FSA-M, BLDG. 61 SO AMSTA-AR-WEL-TL, BLDG. 59 PICATINNY ARSENAL, NJ 07806-5000	1 1 1 1 1 2	COMMANDER U.S. ARMY TANK-AUTMV R&D COMMAND ATTN: AMSTA-DDL (TECH LIBRARY) WARREN, MI 48397-5000	1
DIRECTOR U.S. ARMY RESEARCH LABORATORY ATTN: AMSRL-DD-T, BLDG. 305 ABERDEEN PROVING GROUND, MD 21005-5066	1	COMMANDER U.S. MILITARY ACADEMY ATTN: DEPT OF CIVIL & MECH ENGR WEST POINT, NY 10966-1792	1
DIRECTOR U.S. ARMY RESEARCH LABORATORY ATTN: AMSRL-WM-MB (DR. B. BURNS) ABERDEEN PROVING GROUND, MD 21005-5066	1	U.S. ARMY AVIATION AND MISSILE COM REDSTONE SCIENTIFIC INFO CENTER ATTN: AMSAM-RD-OB-R (DOCUMENTS) REDSTONE ARSENAL, AL 35898-5000	2
COMMANDER U.S. ARMY RESEARCH OFFICE ATTN: TECHNICAL LIBRARIAN P.O. BOX 12211 4300 S. MIAMI BOULEVARD RESEARCH TRIANGLE PARK, NC 27709-2211	1	COMMANDER U.S. ARMY FOREIGN SCI & TECH CENTER ATTN: DRXST-SD 220 7TH STREET, N.E. CHARLOTTESVILLE, VA 22901	1

NOTE: PLEASE NOTIFY COMMANDER, ARMAMENT RESEARCH, DEVELOPMENT, AND ENGINEERING CENTER, BENÉT LABORATORIES, CCAC, U.S. ARMY TANK-AUTOMOTIVE AND ARMAMENTS COMMAND, AMSTA-AR-CCB-O, WATERVLIET, NY 12189-4050 OF ADDRESS CHANGES.